Available online at www.sciencedirect.com
ScienceDirect
International Journal of Machine Tools & Manufacture 47 (2007) 133–140
INTERNATIONAL JOURNAL OF MACHINE TOOLS & MANUFACTURE DESIGN, RESEARCH AND APPLICATION
www.elsevier.com/locate/ijmactool

Study on boring and drilling with vibration cutting

G.-L. Chern*, Jia-Ming Liang

Department of Mechanical Engineering, National Yunlin University of Science and Technology, 123 University Road, Sector 3, Touliu, Yunlin 640, Taiwan

Received 21 August 2005; received in revised form 22 January 2006; accepted 17 February 2006
Available online 18 April 2006

Abstract

In this paper, vibration cutting (VC) has been applied to boring and drilling processes using a vibration device we developed. We analyzed the effect of vibration in boring by investigating the surface roughness of workpiece with the help of Taguchi method and analysis of variance (ANOVA). It has been shown that the utilization of VC in boring improves the surface roughness prominently. The shading-area method we proposed can be employed as a simple and feasible approach for the analysis of burrs in intersecting holes. High-frequency vibration boring can reduce the burr formation in intersecting holes effectively. The experimental results show that the utilization of VC reduces the burrs in intersecting holes noticeably.

Keywords: Vibration cutting; Drilling; Boring; Burr; Intersecting hole

1. Introduction

Vibration cutting (VC) is a technique in which high or low frequency of vibration is superimposed to the cutting tool or the workpiece during a machining operation in order to achieve better cutting performance. This technique had been employed in the precision drilling of wood [1,2] and low carbon steel [3]. The use of low frequency and ultrasonic vibration had been found to be helpful in reducing burr size and prolong tool life in drilling aluminum and glass-fiber reinforced plastics [4,5]. Adachi et al. [4] developed an electro-hydraulic servo-system with a maximum frequency of 100 Hz to produce a low-frequency vibration drilling in aluminum and obtained a decrease in burr size of 5–25%. Onikura et al. [6,7] utilized a piezo-actuator to generate 40 KHz of ultrasonic vibration in the drilling spindle. They found that the use of ultrasonic vibration reduces the friction between chip and rake face, resulting in cutting chips to be thinner, and then considerably reduces the cutting forces. Thus the utilization of VC decreases the hole oversize, reduces the friction between chip and rake face and improves the surface roughness. Chern and Lee [8] proposed a new approach to obtain the desired vibration from the workpiece side. Through extensive experiments with a twist drill size of 0.5 mm, they found that hole oversize, dislocation of the hole center and surface roughness of the drilled hole inner surface could be improved with the increase of vibration frequency and amplitude.

Jin and Murakawa [9] had found that the chipping of the cutting tool can be effectively prevented by applying ultrasonic VC and the tool life can be prolonged accordingly. Takeyama and Kato [5] found that the mean thrust force in drilling can be greatly reduced under ultrasonic VC. Drilling chips are thinner and easier to escape from the drilled hole. Burr formation at the entrance and the exit sides is greatly retarded with the low cutting forces. Thus the overall drilling quality is improved with the employment of VC.

Besides drilling, turning is another field of VC application. Materials like glass with poor machinability are found to be machined effectively with the assistance of VC. The method of ultrasonic VC had been employed to the turning of machinable glass ceramics [10] and soda-lime glass [11]. A surface roughness of 0.03 μm in R_{max} was successfully obtained in face turning of soda-lime glass by applying VC. Ultra-precision ductile cutting of glass could be achieved by applying ultrasonic vibration in the cutting direction.

*Corresponding author. Tel.: +886 5 534 2601 4145; fax: +886 5 531 2062.
E-mail address: cherngl@yuntech.edu.tw (G.-L. Chern).

0890-6955/$ - see front matter © 2006 Elsevier Ltd. All rights reserved.
doi:10.1016/j.ijmachtools.2006.02.017

In general, the steel cannot be machined by diamond tools due to excessive tool wear. But under ultrasonic VC, diamond turning of stainless steel was realized and an optical quality mirror of stainless steel with a surface roughness of 0.026 μm in R_{max} was obtained [12]. Shamoto and Moriwaki [13] proposed an elliptical-vibration-cutting method by introducing synchronized two-directional vibration. Hardened die steel could be machined effectively in their turning experiments [14] with low cutting force, high quality surface and long tool life.

The manufacture of industrial valves often involves drilling and boring operations, generating intersecting holes. One major problem caused is the formation of burrs inside the valves. Deburring of intersecting holes is one of the most difficult deburring tasks faced by many industries. Many deburring processes are not applicable to most intersecting-hole cases, especially when small-diameter drilling is involved. Burrs in intersecting holes may hinder air or liquid flow inside the valve in real application, leading to malfunction or undesirable consequence.

In this paper, a vibration-boring device was designed and fabricated. A piezoelectric actuator is utilized on the end of the boring bar to generate the desired axial vibration. Surface roughness of the workpiece after boring, without and with VC, was investigated. With the help of Taguchi method, influence and contribution ratio of each machining parameter can be determined. Burr formation in intersecting holes was defined as the region shaded by burr within the circular area after drilling and boring. Burr size was then measured through an image-processing software by calculating the number of black pixels in the captured image. Through the experimental results we discussed the effect of VC on boring and drilling.

2. Design and fabrication of vibration-boring device

The basic idea of employing VC on the boring operation is schematically illustrated in Fig. 1. Vibration is applied to the boring bar in the feed direction of the workpiece. To ensure that the boring bar is vibrating in the axial direction of the workpiece, two linear guideways were employed and

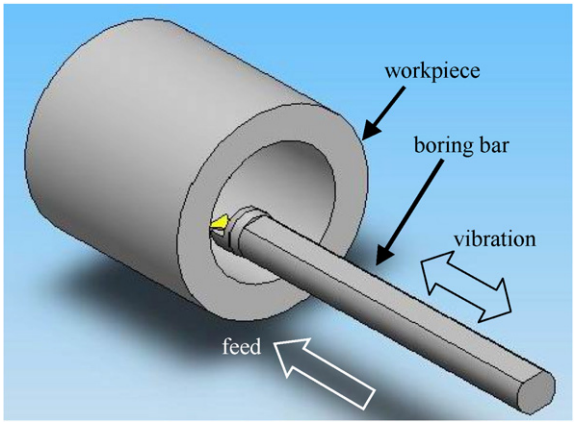

Fig. 1. Vibration cutting for boring operation.

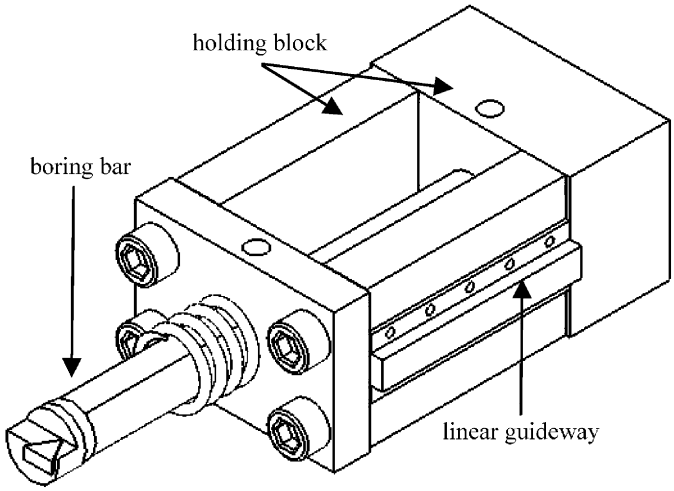

Fig. 2. Linear guideway and holding block.

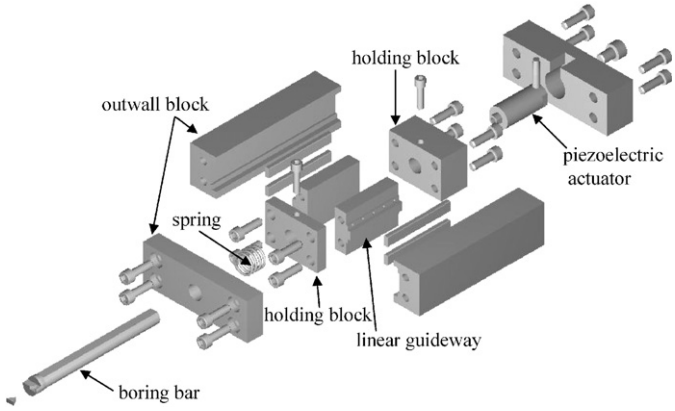

Fig. 3. Vibration-boring device in exploded form.

arranged symmetrically in conjunction with the holding blocks, as shown in Fig. 2. Piezoelectric actuators had been utilized to produce high-frequency vibration in the previous VC researches [6–8,13,14]. Piezoelectric actuators possess the characteristics of fine precision, quick response and large driving force. Thus in this paper we attached a piezoelectric actuator to the end of the boring bar to generate the desired vibration. Four outwall blocks were connected to accommodate the guideways, the holding blocks and the piezoelectric actuator. The whole vibration-boring device is shown in exploded form in Fig. 3. Photo of the device is shown in Fig. 4.

The design for this vibration-boring device is based on the following considerations.

1. Due to the space limitation, the device is designed for the boring bar with a diameter of 12 mm and a length of 150 mm. The boring bar is fastened to the holding block by the screws in Fig. 4.

2. The whole structure must possess enough stiffness to withstand the dynamic loads during the boring operation. Each element of the device is made of stainless steel with high strength to provide enough stiffness.

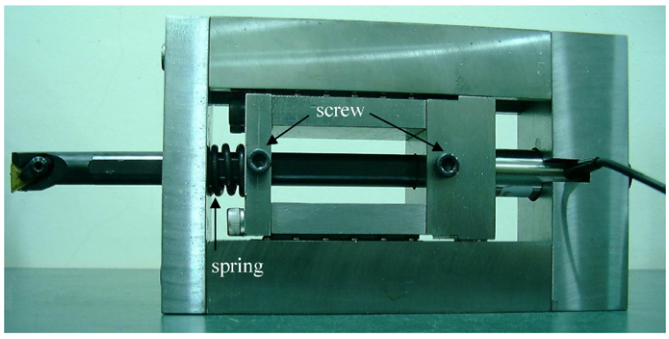

Fig. 4. Photo of vibration-boring device.

3. Piezoelectric actuators operate as capacitive loads. To obtain high-frequency vibration, the power supply must provide enough charging currents. In this research, we used a Physik Instrumente (PI) made piezoelectric actuator (PI P-244.10), cooperated with a high power amplifier (PI P-270.02). The maximum frequency of P-244.10 is 16 kHz. The output voltage of P-270.02 is from 0 to −1000 V. Its peak current is 50 mA and the maximum average output current is 13 mA.

4. The capacities of pushing force and pulling force of P-244.10 are 2000 and 300 N, respectively. Obviously, piezoelectric ceramics can withstand high pushing loads but are brittle and cannot withstand high pulling force. To avoid the possibility of damage occurred in boring due to excessive pulling force, the piezoelectric actuator is preloaded by the spring, as shown in Fig. 4, which is compressed between the outwall block and the holding block. The selection of the spring is based on the boring force involved and the pulling force that can be sustained by the piezoelectric actuator. Thus a steel spring of 1 mm in wire diameter is chosen in this study.

3. Experimental equipment and method

The experimental equipments are described as follows.

Engine lathe (Victor-500 × 1000): to perform boring experiments. Machining center (MC-1050P, Mitsubishi-520AM controller): for the drilling of intersecting-hole experiments. Laser displacement meter (Keyence LC-2430): to measure the amplitude of vibration. The sampling rate of this sensor is 50 kHz. The resolution is 0.01 μm and the laser beam spot is 12 μm. Amplitude of vibration is kept constant at 2 μm throughout the tests.

Toolmakers' microscope (Olympus-STM): to observe the burrs in intersecting holes. It possesses a maximum magnification of 200 times with a resolution of 0.5 μm. Waveform generator (HP-33120A): to provide waveform and frequency for the power amplifier. Surface roughness measuring machine (Talyround, series 2): to measure the surface roughness of the workpiece after boring.

Boring insert: Carbide Depot TPMR221 of 11° clearance, P10 tungsten carbide. Boring bar: Carbide Depot S12M-CTFPR11 with a diameter of 12 mm. Drill: diameter of 1 mm, two flutes, high speed steel (HSS) with an included angle of 118°, a helix angle of 30°, first relieve angle of 15°, and a second relieve angle of 30°. Work material: aluminum alloy (Al 6061-T6) tube with inside diameter of 30 mm and outside diameter of 40 mm. Cutting fluid: mineral oil.

3.1. Vibration-boring experiments

The experiments were conducted on the engine lathe with the vibration-boring device we developed. There were four parameters involved in the experiments and thus in this paper we employed Taguchi method to deal with responses influenced by multi-variables. Taguchi used signal-to-noise (S/N) ratio as the quality characteristics of the choice of parameters. For smaller-the-better characteristic, S/N can be expressed as

$$S/N = -10\log\frac{1}{n}\left(\sum y^2\right),$$

where n is the number of experiments and y is the measured data. The analysis of variance (ANOVA) is then performed to analyze the effect of the process parameters. Based on ANOVA, the contribution ratio of each parameter can be predicted and thus optimal combination of the parameters can be obtained. Detailed description about how to utilize the Taguchi method for the planning of experiments can be found in Refs. [15,16] and is not summarized in this paper.

Since there are four parameters at three levels each, we used the $L_9(3^4)$ orthogonal array to analyze their effects. The process parameters chosen for the vibration-boring experiments are: (**A**) spindle speed, (**B**) vibration frequency, (**C**) feed and (**D**) depth of cut, while the response function is the surface roughness of the drilled hole inner surface. The range and number of levels of the parameters are selected as given in Table 1. The levels of the parameters are chosen based on the results of our preliminary tests and the constraints of the engine lathe we employed. Frequency characteristics of the vibration-boring device were analyzed in the preliminary tests. Its natural frequency was found to be around 10 kHz. The experimental layout for the machining parameters is shown in Table 2. It is noted that only nine experiments are required to study the entire machining parameters using the $L_9(3^4)$ orthogonal array.

Table 1
Machining parameters and their levels in vibration-boring experiments

Level	Param.			
	(**A**) Spindle speed (rpm)	(**B**) Frequency (kHz)	(**C**) Feed (mm/rev)	(**D**) Depth of cut (mm)
1	180	0	0.09	0.04
2	270	1	0.097	0.08
3	310	14	0.105	0.12

Table 2
Experimental layout showing levels of machining parameters in vibration-boring

No.	Param.			
	A	**B**	**C**	**D**
1	1	1	1	1
2	1	2	2	2
3	1	3	3	3
4	2	1	2	3
5	2	2	3	1
6	2	3	1	2
7	3	1	3	2
8	3	2	1	3
9	3	3	2	1

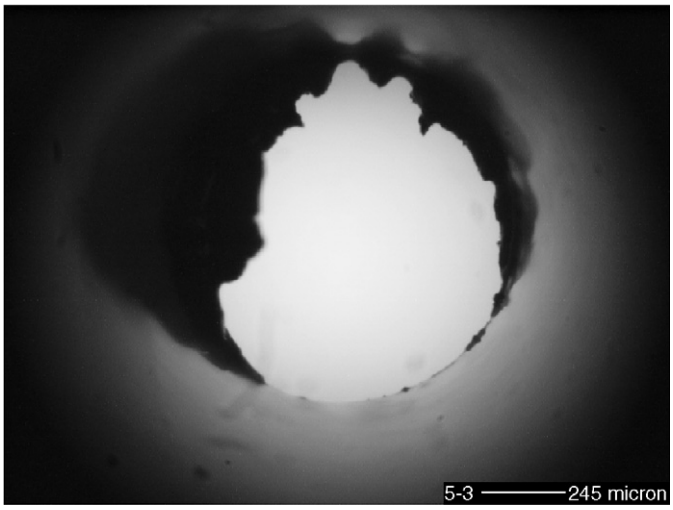

Fig. 5. Photo of burrs in intersecting holes.

3.2. Intersecting-hole experiments

The manufacture of industrial valves often involves drilling a cylindrical tube and then boring its inner wall surface, generating intersecting holes. Burr formation inside the valve becomes a bothersome object to be dealt with. Surface finish of tube workpiece represents the most important machining quality of a boring operation. But for burr formation in intersecting holes, it might not be clear how to choose a quantitative measurement for the research analysis. There are several ways to evaluate the burr formation produced in intersecting holes. The methods of analysis are stated as follows.

1. Maximum burr height: maximum protrusion of burr from the edge of the drilled hole. But if the burr is not quite uniform in shape, such measured value might not be able to represent the real scale of burr formation.

2. Burr weight: weight of burr directly shows the scale of burr formation. To measure the burr weight, one has to carry out deburring first. But collecting all burrs during deburring is a very difficult task. Such method of analysis will be feasible only when a reliable deburring method can be obtained.

3. Burr's "shading area": region shaded by burr within the circular area of drilling. If the burr in intersecting holes is viewed from the axial direction of the drilling process it had undergone, an image like shown in Fig. 5 can be observed. The burr's shading area was then measured through an image-processing software (Matrox Inspector 2.2), as shown in Fig. 6. We crop the photo in Fig. 5 according to the diameter of the drill, which is 1 mm in this research. Now the shading area is measured by counting the black pixels within the captured image. This provides us a quantitative measurement of burr formation in intersecting holes. Since it is more reliable and feasible than the previous two methods, the shading-area approach we proposed will be employed in the following analysis.

The intersecting-hole experiments include two parts: (1) drilling the cylindrical tube workpiece with an HSS drill of diameter 1 mm; (2) boring the inner wall surface of the tube

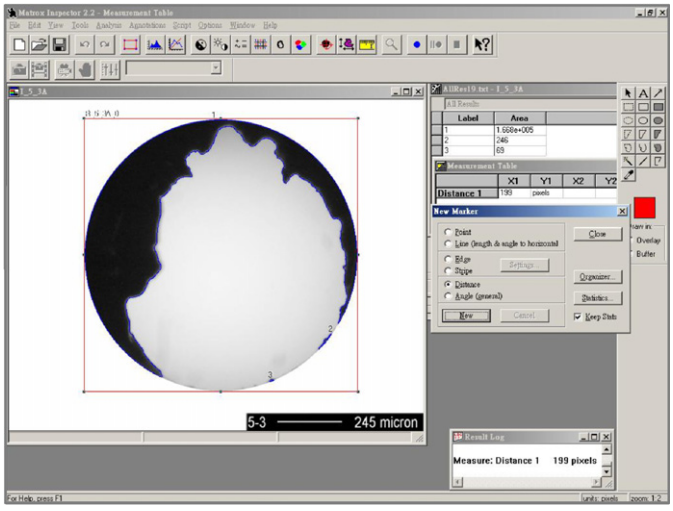

Fig. 6. Image processing of burrs.

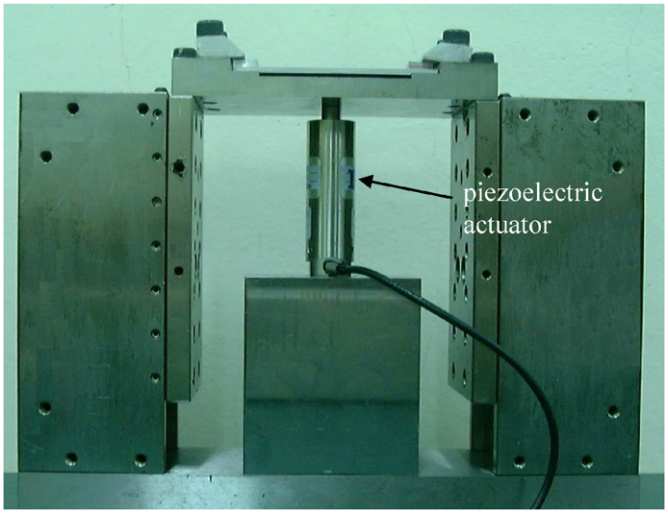

Fig. 7. Photo of vibration-drilling worktable.

Table 3
Machining parameters and their levels in intersecting-hole experiments

Level	Param.			
	(**A**) Frequency in boring (kHz)	(**B**) Frequency in drilling (kHz)	(**C**) Drilling feed (mm/rev)	(**D**) Spindle speed in drilling (rpm)
1	0	0	0.02	1000
2	1	1	0.03	2000
3	14	10	0.04	3000

workpiece. VC is applied to both drilling and boring operations with different vibration devices. Vibration drilling is carried out by employing the vibration worktable which the author had developed [8]. Fig. 7 shows the photo of the vibration-drilling worktable used in the first part of the intersecting-hole experiments. It provides high-frequency vibration in the axial direction, using a piezoelectric actuator (PI P-245.30) coupled by a waveform generator (HP-33120A) and a high power amplifier (PI P-270.02). Two built-in linear guideways are utilized symmetrically to ensure un-axial vertical motion of the worktable.

After drilling through holes, the tube workpiece was machined by the boring operation to complete the intersecting-hole experiments. Again, we used Taguchi method and chose the $L_9(3^4)$ orthogonal array to arrange the experiments. The process parameters selected are: (**A**) vibration frequency in boring; (**B**) vibration frequency in drilling; (**C**) drilling feed; and (**D**) spindle speed in drilling, while the response function is the number of pixels of the captured image. The range and number of levels of the parameters are selected as listed in Table 3. The parameters are chosen based on our previous study in drilling with VC [8], knowing that feed and spindle speed in drilling are important in burr formation. The natural frequency of the vibration worktable was found to be around 13 kHz. The levels of the parameters are chosen based on the results of our preliminary tests and the constraints of the machine tools we employed. The feed, spindle speed and depth of cut in boring are kept at constant of 0.09 mm/rev, 270 rpm and 0.08 mm, respectively. The experimental layout for the machining parameters is the same as shown in Table 2 since the same orthogonal array is chosen.

4. Results and discussions

4.1. Vibration-boring experiments

The objective of the experiments is to optimize the parameters to get better surface roughness in boring with VC. Table 4 shows the actual data measured along with their computed S/N ratio. y is the surface roughness (R_a) measured in μm. The response table for mean S/N ratio is shown in Table 5. We can predict the optimal combination of machining parameters in vibration-boring to be $\mathbf{A_3}$ (310 rpm), $\mathbf{B_2}$ (1 kHz), $\mathbf{C_2}$ (0.097 mm/rev) and $\mathbf{D_1}$ (0.04 mm) by selecting the largest value of S/N ratio for each parameter.

Table 4
Results of vibration-boring experiments and their corresponding S/N ratio

No.	**A**	**B**	**C**	**D**	y	S/N
1	180	0	0.09	0.04	1.494	−3.484
2	180	1	0.097	0.08	1.159	−1.285
3	180	14	0.105	0.12	1.601	−4.089
4	270	0	0.097	0.12	1.566	−3.896
5	270	1	0.105	0.04	1.574	−3.938
6	270	14	0.09	0.08	1.435	−3.139
7	310	0	0.105	0.08	1.652	−4.358
8	310	1	0.09	0.12	1.241	−1.876
9	310	14	0.097	0.04	1.130	−1.062

Table 5
Response table for S/N ratio in vibration boring

	A	**B**	**C**	**D**
1	−2.953	−3.913	−2.833	−2.828
2	−3.658	−2.366	−2.081	−2.927
3	−2.432	−2.764	−4.128	−3.287
Optimal	$\mathbf{A_3}$	$\mathbf{B_2}$	$\mathbf{C_2}$	$\mathbf{D_1}$

Table 6
ANOVA in vibration-boring experiments

Param.	Sum of squares, S	Degree of freedom, f	Variance, V	Contribution ratio, P (%)
A	2.271	2	1.136	17.6
B	3.870	2	1.935	29.9
C	6.434	2	3.217	49.8
D	0.350	2	0.175	2.7
Total	12.925	8		100

The results of ANOVA for the response function, i.e. surface roughness in vibration boring, are given in Table 6. Contribution ratio of each parameter can be seen in the table. The contribution ratios of spindle speed (**A**) and depth of cut (**D**) are 17.6% and 2.7%, respectively. It is found that feed (**C**) has a dominant effect in vibration boring, of almost 50% in contribution ratio. This analysis result is very reasonable since tool mark produced by feed per revolution directly determines the surface roughness in a boring operation.

Vibration frequency (**B**) also has some influence on the surface roughness, of about 30% in contribution ratio. In this study the optimal level of vibration frequency we obtained is $\mathbf{B_2}$ (1 kHz) instead of $\mathbf{B_3}$ (14 kHz). Basic understanding is that when frequency is higher, the performance of VC will be better [7]. This is true only when the cutting tool is not damaged by the high-frequency vibration. Jin and Murakawa [9] pointed out that tool wear is more prominent as frequency increases, as also found by

Chern and Lee [8]. $\mathbf{B_3}$ (14 kHz) might be more susceptible to tool wear in vibration-boring, leading to a poor surface roughness.

To validate the finding of this analysis, confirming experiment was conducted with the optimal level of the machining parameters: $\mathbf{A_3}$, $\mathbf{B_2}$, $\mathbf{C_2}$ and $\mathbf{D_1}$. The measured surface roughness of this optimum combination was 0.717 μm, much lower than the smallest one (1.13 μm) in Table 4. It has been shown that machining parameters set at their optimum levels can ensure significant improvement in the surface roughness in vibration boring.

To investigate the influence of vibration frequency on surface finish produced in boring, some additional experiments were conducted. Fig. 8 shows the variation of surface roughness (R_a and R_{max}) with respect to different vibration frequencies. Spindle speed, feed and depth of cut are 270 rpm, 0.09 mm/rev and 0.04 mm, respectively. It is found that the use of VC in boring does improve the surface roughness. Fig. 9 shows the photos of machined surface after boring, without and with VC. The difference is quite obvious. In Fig. 9(a) we observed clear tool marks and obtained R_a of 1.19 μm without VC. Whereas R_a of 0.73 μm was produced with VC of 1 kHz and the tool marks were almost not distinguishable. Since vibration is imposed in the axial direction, it levels off the tool mark and produces a better surface finish.

4.2. Intersecting-hole experiments

Before discussing the experimental results, burr formation in intersecting holes should be studied first. It is produced by drilling and the following boring operations. Before a drilling process is completed, burr formation initiates due to the lack of material support where the drill exits the workpiece. These uncut materials near the exit side are pushed out and rotated by the bending moment (M) caused from the axial motion of the drill, as shown in Fig. 10(a). Eventually, burrs are created at the exit edge of the drilled hole, as shown in Fig. 10(b).

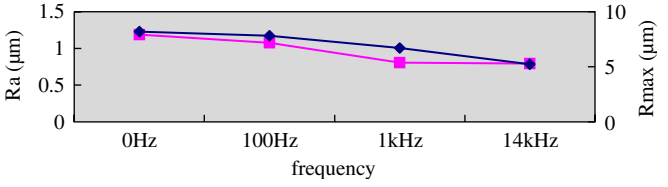

Fig. 8. Variation of surface roughness vs. vibration frequency (270 rpm, 0.09 mm/rev, 0.04 mm).

During the following boring operation, some of those burrs produced by the previous drilling process will be bent to form the final burrs in intersecting holes, as shown in Fig. 11(a). Burrs in region I are most prominent since the drilling burrs in this area form a very large angle with respect to the cutting velocity, V. This angle formed between the workpiece edge and the cutting velocity had been called "in-plane exit angle" and found to be a significant factor in burr formation [17]. Those drilling burrs in region I are easy to rotate with the advancement of the boring tool. Burrs in region III are very few since the feed motion of the boring tool tends to push them around and to be cut away. Fig. 11(b) shows the photo of burrs in intersecting holes.

The objective of the intersecting-hole experiments is to optimize the parameters to get minimum burrs with VC. Table 7 shows the measured number (y) of black pixels of the captured image, using Matrox Inspector 2.2 as in Fig. 6, along with their computed S/N ratio. The response table for mean S/N ratio is shown in Table 8. The optimal combination of machining parameters is $\mathbf{A_3}$ (14 kHz in boring), $\mathbf{B_3}$ (10 kHz in drilling), $\mathbf{C_1}$ (0.02 mm/rev) and $\mathbf{D_3}$ (3000 rpm).

The results of ANOVA for the response function, i.e. black pixels of the captured image, are given in Table 9. It is found that frequency in boring (**A**) has a dominant effect of 71.7% in contribution ratio. The optimal level of **A** is the largest one, 14 kHz. This means that the high-frequency vibration boring can reduce the burr formation in intersecting holes. It is noted that the vibration in the axial direction creates rapid impact on the drilling burrs, causing their breaking off during the boring operation. Thus burr formation is retarded.

To validate the finding of the analysis, confirming experiment was conducted with the optimal level of the machining parameters: $\mathbf{A_3}$, $\mathbf{B_3}$, $\mathbf{C_1}$ and $\mathbf{D_3}$. As expected, the measured number of pixels was 43,606, much lower than

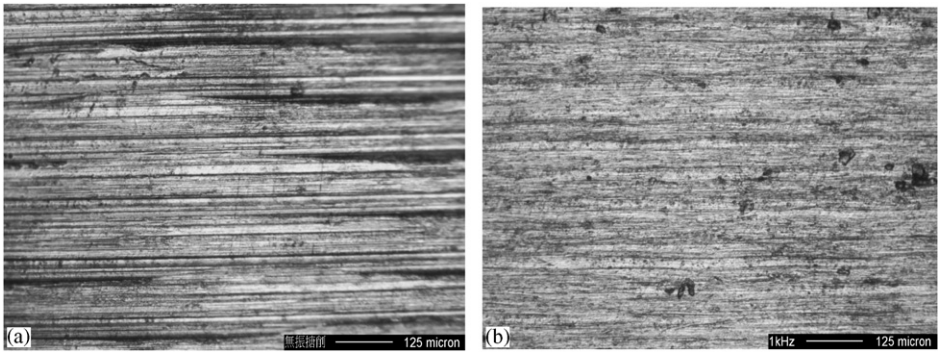

Fig. 9. Photos of machined surface in boring (270 rpm, 0.09 mm/rev, 0.04 mm): (a) without VC; (b) with VC of 1 kHz.

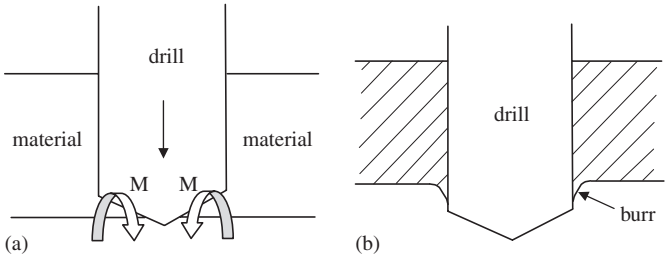

Fig. 10. Burr formation in drilling.

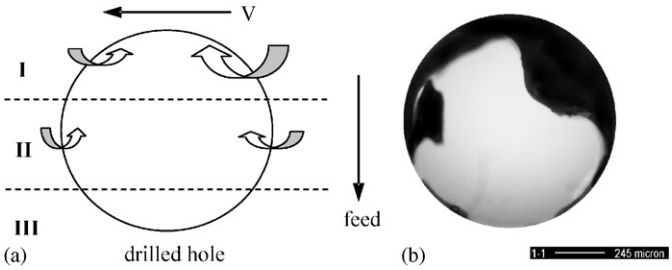

Fig. 11. Burr formation in boring after drilling.

Table 7
Results of intersecting-hole experiments and their corresponding S/N ratio

No.	A	B	C	D	y	S/N
1	0	0	0.02	1000	105,056	−100.43
2	0	1	0.03	2000	185,198	−105.35
3	0	10	0.04	3000	114,025	−101.14
4	1	0	0.03	3000	117,045	−101.37
5	1	1	0.04	1000	167,115	−104.46
6	1	10	0.02	2000	90,910	−99.17
7	14	0	0.04	2000	69,759	−96.87
8	14	1	0.02	3000	60,664	−95.66
9	14	10	0.03	1000	56,003	−94.96

Table 8
Response table for S/N ratio in intersecting-hole experiments

	A	B	C	D
1	−102.307	−99.556	−98.420	−99.951
2	−101.667	−101.824	−100.561	−100.466
3	−95.832	−98.425	−100.824	−99.389
Optimal	$\mathbf{A_3}$	$\mathbf{B_3}$	$\mathbf{C_1}$	$\mathbf{D_3}$

Table 9
ANOVA in intersecting-hole experiments

Param.	Sum of squares, S	Degree of freedom, f	Variance, V	Contribution ratio, P (%)
A	76.388	2	38.194	71.7
B	17.971	2	8.985	16.9
C	10.436	2	5.218	9.8
D	1.741	2	0.871	1.6
Total	106.536	8		100

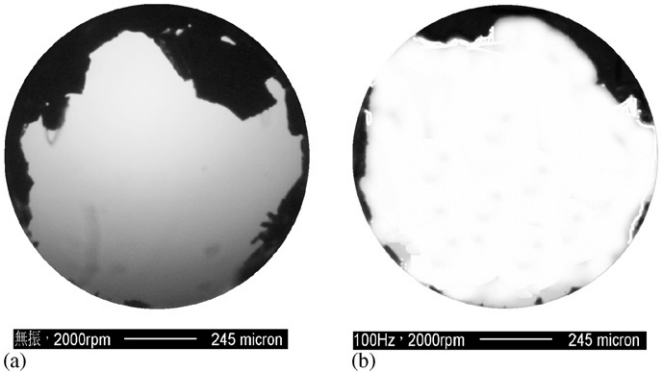

Fig. 12. Photos of burrs in intersecting holes (2,000 rpm, 0.03 mm/rev): (a) without VC; (b) with 100 Hz drilling and 14 kHz boring.

those data in Table 7. Fig. 12 shows the photos of burrs in intersecting holes, without and with VC. Spindle speed and feed in drilling are 2000 rpm and 0.03 mm/rev, respectively. The number of pixels in Fig. 12(a) without VC is 152,162 while such number drops to only 52,973 in Fig. 12(b) with 100 Hz in drilling and 14 kHz in boring. It has been shown that the utilization of VC reduces the burrs in intersecting holes noticeably.

5. Conclusions

1. In this paper, vibration cutting has been applied to boring and drilling processes by the vibration devices we developed. In the vibration-boring experiments, it has been shown that the use of VC improves the surface roughness prominently. Feed has a dominant effect of almost 50% in contribution ratio, while frequency also has influence on the surface roughness of about 30% in contribution ratio based on the Taguchi method and ANOVA. The machining parameters set at their optimum levels can ensure significant improvement in the surface roughness in vibration boring.

2. The shading-area method we proposed can be employed as a simple and feasible approach for analysis of burrs in intersecting holes. In intersecting-hole experiments, we found that high-frequency vibration boring can reduce the burr formation effectively. It has been shown that the utilization of VC reduces the burrs in intersecting holes noticeably.

Acknowledgements

The authors would like to thank the National Science Council in Taiwan ROC for financially supporting this research under contract no. NSC-90-2212-E-224-004.

References

[1] J. Kumabe, T. Sabuzawa, Study on the precision drilling of wood (1st report)—profile analysis of drilled hole, Journal of JSPE 37 (2) (1971) 98–104 (in Japanese).

[2] J. Kumabe, T. Sabuzawa, Study on the precision drilling of wood (2nd report)—drilling force and its accuracy, Journal of JSPE 38 (5) (1972) 456–461 (in Japanese).
[3] T. Koyama, K. Adachi, K. Murakami, Study on vibratory drilling (2nd Report)—comparison of conventional drilling with vibratory drilling, Journal of JSPE 43 (1) (1977) 55–60 (in Japanese).
[4] K. Adachi, N. Arai, S. Harada, K. Okita, S. Wakisaka, A study on burr in low frequency vibratory drilling—drilling of aluminum, Bulletin of JSPE 21 (4) (1987) 258–264.
[5] H. Takeyama, S. Kato, Burrless drilling by means of ultrasonic vibration, Annals of CIRP 40 (1) (1991) 83–86.
[6] H. Onikura, O. Ohnishi, J.H. Feng, T. Kanda, T. Morita, U. Bopp, Effects of ultrasonic vibration on machining accuracy in microdrilling, International Journal of JSPE 30 (3) (1996) 210–216.
[7] H. Onikura, O. Ohnishi, Drilling mechanisms in ultrasonic-vibration assisted microdrilling, Journal of JSPE 64 (11) (1998) 1633–1637 (in Japanese).
[8] G.L. Chern, H.J. Lee, Using workpiece vibration cutting for microdrilling, International Journal of Advanced Manufacturing Technology 27 (7) (2006) 688–692.
[9] M. Jin, M. Murakawa, Development of a practical ultrasonic vibration cutting tool system, Journal of Materials and Processing Technology 113 (2001) 342–347.
[10] H. Weber, J. Herberger, R. Pilz, Turning of machinable glass ceramics with an ultrasonically vibrated tool, Annals of CIRP 33 (1) (1984) 85–87.
[11] T. Moriwaki, E. Shamoto, K. Inoue, Ultraprecision ductile cutting of glass by applying ultrasonic vibration, Annals of CIRP 41 (1) (1992) 141–144.
[12] T. Moriwaki, E. Shamoto, Ultraprecision diamond turning of stainless steel by applying ultrasonic vibration, Annals of CIRP 40 (1) (1991) 559–562.
[13] E. Shamoto, T. Moriwaki, Study on elliptical vibration cutting, Annals of CIRP 43 (1) (1994) 35–38.
[14] E. Shamoto, T. Moriwaki, Ultraprecision diamond cutting of hardened steel by applying elliptical vibration cutting, Annals of CIRP 48 (1) (1999) 441–444.
[15] P.M. George, B.K. Raghunath, L.M. Manocha, A.M. Warrier, EDM machining of carbon-carbon composite—a Taguchi approach, Journal of Materials and Processing Technology 145 (2004) 66–71.
[16] J.A. Ghani, I.A. Choudhury, H.H. Hassan, Application of Taguchi method in the optimization of end milling parameters, Journal of Materials and Processing Technology 145 (2004) 84–92.
[17] G.L. Chern, D.A. Dornfeld, Burr/breakout model development and experimental verification, Journal of Engineering and Material Technology 118 (1996) 201–206.